# ISTITUTO NAZIONALE DI RICERCA METROLOGICA
# Repository Istituzionale

International comparison on SST and Epstein measurements in grain-oriented Fe-Si sheet steel

(Article begins on next page)

02 May 2024

# International comparison on SST and Epstein measurements in grain-oriented Fe-Si sheet steel

C. Appino[1], E. Ferrara[1], F. Fiorillo[1*], L. Rocchino[1], C. Ragusa[2], J. Sievert[3], T. Belgrand[4], C. Wang[5], P. Denke[6], S. Siebert[6], Y. Norgren[7], K. Gramm[7], S. Norman[8], R. Lyke[8], M. Albrecht[9], X. Zhou[10], W. Fan[11], X. Guo[12], M. Hall[13]

*[1]INRIM, Torino, Italy, [2]Politecnico di Torino, Italy, [3]PTB (former affiliation), Braunschweig, Germany, [4]TKES, Isbergues, France, [5]TKES, Gelsenkirchen, Germany, [6]BROCKHAUS Messtechnik, Lüdenscheid, Germany, [7]ABB, Ludvika, Sweden, [8]AK Steel, Middletown, USA, [9]PTB, Braunschweig, Germany, [10]BAOSTEEL, Shanghai, China, [11]NIM, Beijing, China, [11]WISCO, Wuhan, China, [13]NPL,Teddington, UK.*

**Abstract**

We discuss the results of an international comparison regarding the measurement of magnetic power loss and apparent power between 20 Hz and 100 Hz at magnetic polarization values ranging between 1.3 T and 1.8 T in grain-oriented steel (GO) sheets using the Single Sheet Testing (SST) and Epstein methods. This exercise, carried out in the framework of the activity of Joint Working Group IEC 68/WG1- ISO/TC17/WG16, was aimed at a solid assessment of the degree of reproducibility of the SST method, under its prospective adoption in the industrial practice as a reference method for the specifications of grain-oriented alloys. Five different types of Fe-Si GO alloys were circulated among eleven different laboratories of metrological institutes and industry. The statistical analysis of the results shows close reproducibility properties of the SST and Epstein methods. It is obtained, in particular, that the power loss figures, measured by the participants at 50 Hz and the aforementioned peak polarization values are distributed around their reference value with relative standard deviation $\sigma(P)_{\text{SST}} = 0.88$ % and $\sigma(P)_{\text{Epst}} = 0.82$ % for SST and Epstein, respectively. It is obtained $\sigma(S)_{\text{SST}} = 2.20$ % and $\sigma(S)_{\text{Epst}} = 2.15$ % for the apparent power. For the industrially relevant case of polarization $J_p = 1.7$ T in the high-permeability P-type grades, these quantities amount to $\sigma(P)_{\text{SST}} = 0.48$ %, $\sigma(P)_{\text{Epst}} = 0.80$ %. By restricting the comparison to the European metrological laboratories (INRIM, NPL, PTB), the overall distributions narrow to $\sigma(P)_{\text{SST}} = 0.42$ %, $\sigma(P)_{\text{,Epst}} = 0.55$ %, $\sigma(S)_{\text{SST}} = 1.19$ %, and $\sigma(S)_{\text{Epst}} = 0.82$ %. A qualitative interpretation of the main physical mechanisms and the measuring features underlying the lab-to-lab dispersion of the SST and Epstein results is discussed in this paper. It is concluded that the combination of good reproducibility and simple practical implementation make the SST method totally appropriate as a reference method for the definition of the material quality in the specification standards.

Keywords: Grain-oriented Fe-Si, Single Sheet Testing method, Epstein method, Measurement comparisons.

---------------------------------------

*[*]Corresponding author. Tel. +39 0113919836; Fax. +39 0113919834; e-mail: f.fiorillo@inrim.it*

# 1. Introduction

The magnetic characteristics of electrical steel are significant in two regards. First, they are decisive for the possible applications of the material. Secondly, the magnetic loss performance is relevant to material costs and the efficiency of energy transformation, i.e. the economic and environmental aspects. The Epstein method [1] and the Single Sheet Tester (SST) method [2] are the two standardized methods in force for the measurement of the magnetic properties of electrical steel sheets at power frequencies. They realize a closed magnetic configuration either by arranging 30 mm × 300 mm test strips into a square (Epstein frame) or placing a 500 mm × 500 mm sheet inside a double-C laminated yoke (SST, see Ref. [3] for details). The present IEC standard for SST testing [2], laid upon the results of many investigations and interlaboratory comparisons [4-7], does not contemplate calibration by reference to the Epstein measurements. It has been recognized that both Epstein and SST provide systematic contributions to the measurement uncertainty, which can cause in grain-oriented alloys differences of up to 10% between the correspondingly obtained specific total power loss values $P_s$ at polarization $J_p = 1.7$ T. These differences were found to derive to a greater extent from a negative Epstein contribution and, to a smaller extent, from a positive SST contribution [3]. Epstein testing is at present still defined as the sole reference method for the determination of the material quality in the specification standards, although the SST method features practical simplicity (no stress-release annealing of sample) and applicability also to highest grade materials (domain refined grades). Consequently, there is strong demand by an increasing part of the industry for including SST reference values in the specification standards. For this reason, the Epstein to SST relationship was recently subjected to intense investigation [8-10]. It turned out that this relation is affected by large uncertainties, the combination of systematic effects, intrinsic to the specific nature of the SST and Epstein magnetic circuits, and many statistical components, depending on material type, electronic apparatus, measurement parameters, etc.. For example, a systematic change of the loss performance of large-grained materials (high-permeability grain-oriented Fe-Si) can occur when cut into 30 mm wide strips for Epstein testing, while additional dispersion can be caused by different annealing treatments. It is then apparent that the route to SST-based reference loss values should not hinge upon a direct link to the Epstein method.

A number of interlaboratory exercises, performed at 50 Hz/60 Hz on grain-oriented alloys, provided comparable reproducibility behaviours of Epstein and SST measurements [4,11,12]. On the other hand, a recent comparison on grain-oriented alloys involving six manufacturers has brought to light a wide dispersion of the SST to Epstein power loss ratio [10], somewhat larger and partly contradictory with respect to a previous experimental assessment of this quantity [8]. If possible differences in the preparation process of the Epstein strips are further considered, broader scatter of the results associated with the circulation of the same samples among laboratories is to be expected. An extended and methodically stringent round robin exercise on the power loss and apparent power measurement on grain-oriented Fe-Si laminations with the SST method, covering a range of material grades, frequencies, and peak polarization values was then promoted by the IEC Technical Committee 68, in order to definitely assess the SST reproducibility features

and provide solid background for its adoption as a reference method. Four metrological institutes and seven industrial laboratories took part in the comparison. They are listed in Table 1. Besides the 500 mm × 500 mm sheets, Epstein strips taken from the same batch, were circulated and tested at the same time, thereby providing further information on the Epstein to SST relationship. The material was supplied by Thyssenkrupp Electrical Steel, Isbergues. The magnetics laboratory of the Istituto Nazionale di Ricerca Metrologica (INRIM) acted as pilot laboratory. In this paper we summarize and discuss the results of this measuring exercise, focusing on the distribution of the SST values obtained by the participating laboratories around the reference values and the dependence of the standard deviation on magnetizing frequency and peak polarization. Comparison will be made with the accompanying Epstein results and the related distributions.

## 2. Circulation of the samples and measurement procedure

Two conventional grain-oriented (CGO) and three high-permeability (HGO) Fe-Si alloys, taken from the production line, were delivered, both as 500 mm × 500 mm SST plates and 300 mm × 30 mm Epstein strips, by Thyssenkrupp Electrical Steel Isbergues (TKES) to the pilot laboratory (INRIM). Mass and cross-sectional area of the individual SST sheets and of the Epstein samples (32 strips for each alloy) were determined by TKES and their values were adopted by all partners. The circulation of the samples (listed in Table 2) took about one year, at the end of which INRIM repeated the whole set of measurements. The second round of measurements by INRIM had the scope of verifying any possible damage to the samples or drift of the material properties upon circulation. Since the repeated measurements of INRIM are assumed to be correlated with those made at the start, they were excluded from the statistical analysis (they are nevertheless available for any further analysis). The following quantities were measured, according to the IEC 60404-3 (SST 92) and IEC 60404-2 (Epstein) standards, at the frequencies $f$ = 20, 40, 50, 60, 80, 100 Hz and peak polarization values $J_p$ = 1.3, 1.5, 1.7, 1.8 T: power loss $P$, apparent power $S$, associated peak value of the fieldstrength $H_p$, and polarization $J_{800}$ for $H$ = 800 A/m. The measurements were carried out, following demagnetization at 50 Hz, at the temperature 23 °C ± 2 °C. Repeatability was checked, for all the previous quantities, at 50 Hz by making five successive measurements without intervening demagnetization. INRIM gathered all the results by the partners, which were assumed to have appropriate traceability of measurements to the SI standards, and performed the related statistical analysis.

## 3. Results and analysis of the measured quantities.

Data analysis in a comparison exercise basically aims at the determination of a reference value for each measured quantity and its expanded uncertainty, which identifies the 95 % confidence level around such value [13, 14]. In particular, by denoting with $y_i$ the best estimate of the i-th laboratory and with $u_c(y_i)$ the related combined uncertainty, the reference value is obtained as a weighted mean

$$<< y >> = \sum_{i=1}^{N} g_i y_i$$, obtained by averaging the best estimates $y_i$ of the $N$ laboratories once they have

been assigned a weight factor $g_i \propto (1/u_c^2(y_i))$ [3]. The main systematic contributions to $u_c(y_i)$ are here identified with the calibration of the $H$ and $B$ channels, imperfections in the magnetic circuit and the arrangement of the samples, uncontrolled stresses, and spurious phase shifts between primary and secondary signals. It is noted that all participants adopt the very same cross-sectional area of the sample and the systematic effect due to the specific non-ideal nature of the Epstein and SST circuit, identical for all labs, can be ignored. In the present comparison, however, a good number of laboratories could not provide defined uncertainty values with their best estimates. The unweighted mean $< y >= \sum_{i=1}^{N} y_i / N$ was consequently assumed as the reference value. This is an acceptable option, because the objective of the exercise is more one of assessing the measurement reproducibility than one of providing a 95 % level of confidence interval around the true value of the investigated quantity. We shall thus define in the following the degree of reproducibility of the SST and Epstein methods through the dispersion of the best estimates $y_i$ around $<y>$ and the associated standard deviation $\sigma(y)$. By defining the reproducibility $R(y)$ as the standard deviation of the lab-to-lab differences, it is obtained $R(y) = \sqrt{2} \cdot \sigma(y)$. Given our inability to identify the outliers from knowledge of weighted mean and calculation of the so-called normalized error [14], it was decided to exclude the best estimates falling outside a $\pm 2\sigma$ interval around $<P>$ (or $<S>$). We show in Fig. 1 and Fig. 2 two examples of scattering of results around the reference values $<P>$ and $<S>$. They refer to CGO and HGO samples, respectively. The labeling order of the laboratories does not correspond to that of Table 1. The source of any specific figure of $P$ and $S$ is kept undisclosed, but for the pilot laboratory PL. Table 3 provides the whole set of reference values $<P>$ and $<S>$ at 50 Hz, where it is confirmed the usual finding of SST figures higher than the Epstein ones. It is also confirmed, according to previous literature [10], that the ratio $<P_{SST}>$ / $<P_{Epst}>$ exhibits large scattering upon different samples, as illustrated in Fig. 3. The reference values for $J_{800}$, the polarization at $H = 800$ A/m, and the related standard deviations are given in Table 4.

We have considered the whole matrix of reference values $<P>$ and $<S>$ at 50 Hz shown in Table 3 and the associated distributions of the laboratories best estimates $P_i$ and $S_i$. In particular, the relative differences $\delta(P_i) = (P_i - <P>) / <P>$ and $\delta(S_i) = (S_i - <S>) / <S>$ for each sample and $J_p$ value have been taken and the standard deviation of their distributions has been derived. The SST and Epstein distributions, showing close behaviors, approximately fit a Gaussian function. We obtain the standard deviations $\sigma(P)_{SST} = 0.88$ % and $\sigma(P)_{Epst} = 0.82$ % for the power loss, $\sigma(S)_{SST} = 2.20$ % and $\sigma(S)_{Epst} = 2.15$ % for the apparent power. It is remarked, comparing the histograms of Fig. 4 and Fig. 5, the improved reproducibility of the results provide by the European metrological laboratories (INRIM, NPL, PTB). The standard deviations associated with these narrower distributions are $\sigma(P)_{SST} = 0.42$ %, $\sigma(P)_{,Epst} = 0.55$ %, $\sigma(S)_{SST} = 1.19$ %, and $\sigma(S)_{Epst} = 0.82$ %. Again, little difference is observed between SST and Epstein dispersions. It is stressed that the present results favourably compare with the outcomes of a comparison carried out on 15 grain-oriented steel sheets by the same labs in the year 2000 at $J_p = 1.5$ T and $J_p = 1.7$ T, as illustrated in Table 5.

4

The overall distributions of the differences $\delta(P_i)$ and $\delta(S_i)$ at 50 Hz given in Fig. 4 can be decomposed in the sub-ensembles associated with the different $J_p$ values, to achieve the evolution of the standard deviations $\sigma(P)$ and $\sigma(S)$ versus $J_p$. Fig. 6 shows, for example, the dispersion of the power loss estimates versus $J_p$. This figure, besides confirming the relatively close behaviours of SST and Epstein power loss dispersions, shows that the minimum standard deviation $\sigma(P)$, of the order of 0.5 %, is obtained for the SST measurements at $J_p = 1.7$ T. This happens to be the condition where also the SST apparent power attains minimum dispersion. Fig. 7 provides an overall view of the evolution of $\sigma(P)$ and $\sigma(S)$ versus frequency and peak polarization. While it can be generally observed that, consistent with the results shown in Fig. 4, the standard deviations $\sigma(P)_{SST}$ and $\sigma(P)_{Epst}$ do not sensibly differ across the whole $f$ and $J_p$ range (at most $|\sigma(P)_{SST} - \sigma(P)_{Epst}| \sim 0.4$ %), it appears that both of them tend to show a more or less shallow minimum at intermediate $J_p$ values. In this comparison, where the cross-sectional area of the sample is fixed by definition, the main factors affecting the lab-to-lab reproducibility belong either to the nature of the magnetization process and the features of the magnetic circuit or to the properties of the electronic setup, that is its signal handling capabilities and the quality of the calibration procedures. At low induction values the stochastic behaviour of the magnetization process tends to worsen the reproducibility. This effect is more important at low frequencies, where the homogenizing effect of eddy currents is lower. The moderate rise of $\sigma(P)_{SST}$ and $\sigma(P)_{Epst}$ beyond $J_p = 1.7$ T is ascribed instead to different performances of the different wattmeters in dealing with the strong non-linearity of the hysteresis loops and the small phase shift (a few degrees) between field (fundamental harmonic) and induction. This is actually assumed to be one main reason for the dramatic increase of $\sigma(S)_{SST}$ beyond $J_p = 1.7$ T and of $\sigma(S)_{Epst}$ beyond $J_p = 1.5$ T. Because of the large drop of the differential permeability at high inductions, a small uncertainty on $J_p$ (i.e peak induction $B_p \cong J_p$) is reflected in a large uncertainty of $H_p$ and affects the uncertainty associated with the apparent power

$S = \widetilde{H}(\dfrac{d\widetilde{B}}{dt})$ [VA/m³] via the rms field value $\widetilde{H}$. We can express the relative uncertainty on the

measured $H_p$ value for imposed $J_p$ value as $\dfrac{u(H_p)}{H_p} = \sqrt{(\dfrac{u_0(H_p)}{H_p})^2 + (\dfrac{dH_p}{dJ_p})^2 \cdot (\dfrac{J_p}{H})^2 \cdot (\dfrac{u(J_p)}{J_p})^2}$ , where

$\dfrac{u_0(H_p)}{H_p}$ lumps the $J_p$- independent contributions ($J_p \cong B_p$). For the practical case of a CGO sheet at high induction (1.7 T $\leq J_p \leq$ 1.8 T), the relative differential permeability is $(1/\mu_0) \cdot (dB/dH) \sim 250$ and $(1/\mu_0) \cdot (B/H) \sim 4000$. Assuming $\dfrac{u_0(H_p)}{H_p} = 0.5$ % and $\dfrac{u(J_p)}{J_p} = 0.5$ %, we obtain $\dfrac{u(H_p)}{H_p} \sim 7$ %.

Looking again at Fig. 7, it is noted how $\sigma(S)_{SST}$ passes through a minimum value at $J_p = 1.7$ T, while $\sigma(S)_{Epst}$ monotonically decreases by decreasing $J_p$. These behaviours demonstrate that a substantial reproducibility of the strips arrangement and the related magnetostatic effects at the corners can be achieved with the Epstein frame, while the inevitable, though small, discontinuities of the magnetic

circuit with the SST configuration will create different distributions of the free poles at the yoke-sheet interface with different yokes and in different labs. The involved demagnetizing fields, estimated from the slope of the quasi-static SST hysteresis loops around the coercive field, are of the order of a few A/m at 1 T. They will expectedly interfere with the shape of the low induction loops (i.e. with the related apparent power), the lower the induction the higher the effect, much less with their area (i.e. the power loss). Fig. 8 clearly shows how the lab-to-lab scatter of the SST peak field values at $J_p$ = 1.3 T and $f$ = 50 Hz largely overcomes the corresponding scatter of the Epstein peak field, which is mirrored by the opposite trends of $\sigma(S)_{SST}$ and $\sigma(S)_{Epst}$ on decreasing $J_p$ below $J_p$ = 1.7 T. It is observed that a same analysis made at $J_p$ = 1.7 T and $J_p$ = 1.8 T does not show significant differences between the SST and Epstein lab-to-lab fluctuations of $H_p$ (see Fig. 8b), while bringing to light much larger scatter. This is fully consistent with the high-induction trend of $\sigma(S)_{SST}$ and $\sigma(S)_{Epst}$ shown in Fig. 7.

## 4. Conclusions

An extended international comparison on the measurement of power loss and apparent power in grain-oriented steel sheets has demonstrated close reproducibility of results obtained by the Single Sheet Testing (SST) and Epstein measuring methods. In particular, the dispersion of the laboratories best estimates at 50 Hz exhibits, with both methods, a standard deviation lower than 1 % for the power loss and slightly higher than 2 % for the apparent power across the peak polarization range 1.3 T – 1.8 T. Narrower distributions are obtained by restricting the comparison to the European metrological laboratories. These results solidly support the proposed adoption of SST as an independent method, not traceable to the Epstein method, in the definition of the specification standards of grain-oriented materials. It is also confirmed by the present measurements that the SST to Epstein power loss ratio suffers large scattering across the investigated steel sheets, casting doubts on the use of such a ratio to grade the SST tested materials in terms of reconstructed Epstein figures.

The main sources of lab-to-lab scattering of the power loss figures are identified with the stochastic properties of the magnetization process at low inductions and the resolution and signal handling capability of the different measuring setups at high inductions. It is observed that minimum dispersion is attained at 50 Hz – 60 Hz and $J_p$ = 1.7 T, the testing regime typically adopted for the standard characterization of the grain-oriented alloys, where the industrial setups are optimized. The local discontinuities of the magnetic circuit at the yoke-sample interface, fluctuating from lab to lab, may somewhat contribute to the widening of the SST power loss distribution towards the lower $J_p$ values, but they are especially detrimental for the dispersion of the apparent power figures, given the pre-eminent role of the associated demagnetizing fields. The drop of the differential permeability at high inductions, beyond about $J_p$ = 1.7 T, engenders a large uncertainty in the corresponding determination of the peak field value, besides posing resolution problems in the integration process. This becomes a main reason for the increase of the dispersion of the laboratory estimates at very high inductions, especially dramatic for the apparent power.

**References**

[1]  IEC Standard Publication 60404-2 ed.3.1, Magnetic materials - Part 2: Methods of measurement of the magnetic properties of electrical steel sheet and strip by means of an Epstein frame (Geneva: IEC Central Office, 2008).

[2]  IEC Standard Publication 60404-3 ed2.2, Magnetic materials - Part 3: Methods of measurement of the magnetic properties of electrical steel strip and sheet by means of a single sheet tester (Geneva: IEC Central Office, 2010).

[3]  F. Fiorillo, *Measurement and Characterization of Magnetic Materials*, Elsevier-Academic Press, 2004.

[4]  A.E. Drake and C. Ager, BCR Report EUR 12377 EN (Commission of the European Community, Bruxelles, 1989).

[5]  J. Sievert, M. Binder, and L. Rahf, On the reproducibility of single sheet testers: comparison of different measuring procedures and SST designs, *Anales de Fisica-B*, **86** (1990), 76-78.

[6]  T. Nakata, K. Fujiwara, M. Nakano, and T. Kayada, Influence of yoke construction on magnetic characteristics of single sheet testers, *IEEE Transl. J. Magn. Japan* **5** (1990) 618-624.

[7]   T. Nakata, N. Takahashi, K. Fujiwara, M. Nakano, and T. Kayada, Effects of eddy currents in the specimen in a single sheet tester on measurement errors, *IEEE Trans. Magn.* **26** (1990) 1641-1643.

[8]  J. Sievert, The measurement of magnetic properties of electrical sheet steel. Survey of methods and standards, *J. Magn. Magn. Mater.* **215-216** (2000), 647-651.

[9]  J. Sievert and H. Ahlers, Epstein to SST relationship-statistical rather than deterministic, *Przeglad Elektrotechniczny*, **87** (2011), 17-19.

[10] J. Sievert, T. Belgrand, D. Fox, X. Guo, T. Kochmann, R. Lyke, C. Wang, and X. Zhou, New data on the Epstein to Single Sheet Tester relationship, *Przeglad Elektrotechniczny*, **89** (2013), 1-3.

[11] R. Girgis, K. Gramm, J. Sievert, and M.G. Wickramasekara, The single sheet tester. Its acceptance, reproducibility, and application issues on grain-oriented steel, *J. Phys. IV (France)*, **8** (1998), 729-732.

[12] J. Sievert, H. Ahlers, F. Fiorillo, L. Rocchino, M. Hall, and L. Henderson, Magnetic measurements on electrical steels using Epstein and SST method, *PTB-Bericht,* **E-74** (2001), 1-28.

[13] JCGM, *Evaluation of Measurement Data-Guide to the Expression of Uncertainty in Measurement*, September 2008 (http://www.bipm.org/en/publications/guides/gum.html).

[14] R. Thalmann, EUROMET key comparison: cylindrical diameter standards, *Metrologia*, **37** (2000), 253-260.

Table 1 -    The participating laboratories. The numerical labels appended in the following diagrams do not correspond to the order of this list.

| Laboratory, address |
| --- |
| INRIM, Istituto Nazionale di Ricerca Metrologica, Torino, Italy (pilot laboratory). |
| PTB, Physikalisch-Technische Bundesanstalt, Braunschweig, Germany. |
| NPL, National Physical Laboratory, Teddington, UK. |
| NIM, National Institute of Metrology, Beijing, China. |
| TKES, ThyssenKrupp Electrical Steel, Isbergues, France. |
| TKES, ThyssenKrupp Electrical Steel, Gelsenkirchen, Germany. |
| Brockhaus Messtechnik, Lüdenscheid, Germany. |
| ABB, Ludvika, Sweden. |
| AK Steel, Middletown, USA. |
| Baosteel, Shangai, China. |
| WISCO, Wuhan, China. |

Table 2 – The circulated grain-oriented Fe-Si test samples.

| Code | Type | Nominal density (kg/m$^3$) | Thickness (mm) |
|---|---|---|---|
| Sample #1 | CGO | 7650 | 0.254 |
| Sample #2 | CGO | 7650 | 0.289 |
| Sample #3 | HGO | 7650 | 0.260 |
| Sample #4 | HGO | 7650 | 0.286 |
| Sample #5 | HGO laser scribed | 7650 | 0.217 |

Table 3 – The reference values at 50 Hz for the power loss $P$ and the apparent power $S$.

| Sample | $J_p$ (T) | $<P_{SST}>$ (W/kg) | $<P_{Epst}>$ (W/kg) | $<S_{SST}>$ (VA/kg) | $<S_{Epst}>$ (VA/kg) |
|--------|-----------|--------------------|---------------------|---------------------|----------------------|
| #1 |     | 0.579 | 0.560 | 0.764 | 0.696 |
| #2 |     | 0.619 | 0.594 | 0.786 | 0.714 |
| #3 | 1.3 | 0.509 | 0.501 | 0.611 | 0.567 |
| #4 |     | 0.580 | 0.562 | 0.688 | 0.632 |
| #5 |     | 0.442 | 0.438 | 0.700 | 0.657 |
| #1 |     | 0.801 | 0.774 | 1.210 | 1.080 |
| #2 |     | 0.85  | 0.819 | 1.220 | 1.092 |
| #3 | 1.5 | 0.682 | 0.677 | 0.840 | 0.771 |
| #4 |     | 0.779 | 0.753 | 0.975 | 0.862 |
| #5 |     | 0.597 | 0.589 | 1.070 | 1.002 |
| #1 |     | 1.189 | 1.132 | 3.410 | 2.730 |
| #2 |     | 1.232 | 1.181 | 3.270 | 2.640 |
| #3 | 1.7 | 0.922 | 0.906 | 1.370 | 1.170 |
| #4 |     | 1.050 | 1.010 | 1.530 | 1.320 |
| #5 |     | 0.824 | 0.799 | 1.950 | 1.710 |
| #1 |     | 1.540 | 1.466 | 11.28 | 8.290 |
| #2 |     | 1.562 | 1.497 | 10.71 | 8.570 |
| #3 | 1.8 | 1.129 | 1.107 | 2.490 | 1.840 |
| #4 |     | 1.287 | 1.228 | 2.850 | 2.160 |
| #5 |     | 1.047 | 1.018 | 3.640 | 3.20  |

Table 4 –  Reference values at 50 Hz of the polarization at $H = 800$ A/m $J_{800}$ and standard deviation of the distribution of the laboratories best estimates.

| Sample | $J_{800,SST}$ (T) | $\sigma_{SST}$ (%) | $J_{800,Epst}$ (T) | $\sigma_{Epst}$ (%) |
|--------|-------------------|--------------------|--------------------|---------------------|
| #1 | 1.818 | 0.337 | 1.840 | 0.411 |
| #2 | 1.822 | 0.334 | 1.837 | 0.363 |
| #3 | 1.920 | 0.347 | 1.934 | 0.338 |
| #4 | 1.913 | 0.337 | 1.927 | 0.273 |
| #5 | 1.905 | 0.369 | 1.907 | 0.305 |

Table 5 – Relative standard deviations of 50 Hz power loss $P$ and apparent power $S$ distributions around their reference values, obtained by comparing the measurements of INRIM, PTB, and NPL. The results obtained by an exercise on 15 different grain-oriented steel sheets performed in the year 2000 [12] are compared with the present measurements.

| $J_p$ (T) | $\sigma(P)_{SST,2000}$ (%) | $\sigma(P)_{SST,2014}$ (%) | $\sigma(P)_{Epst,2000}$ (%) | $\sigma(P)_{Epst,2014}$ (%) | $\sigma(S)_{SST,2000}$ (%) | $\sigma(S)_{SST,2014}$ (%) | $\sigma(S)_{Epst,2000}$ (%) | $\sigma(S)_{Epst,2014}$ (%) |
|---|---|---|---|---|---|---|---|---|
| 1.5 | 0.61 | 0.33 | 0.50 | 0.55 | 1.15 | 1.00 | 0.39 | 0.55 |
| 1.7 | 0.75 | 0.43 | 0.62 | 0.55 | 2.18 | 1.11 | 1.31 | 1.08 |

**Figure captions**

Table 1 -      The participating laboratories. The numerical label appended in the following diagrams does not correspond to the order of this list.

Table 2 – The circulated grain-oriented Fe-Si test samples.

Table 3 – The reference values at 50 Hz for the power loss $P$ and the apparent power $S$.

Table 4 – Reference values at 50 Hz of the polarization at $H = 800$ A/m $J_{800}$ and standard deviation of the distribution of the laboratories best estimates.

Table 5 – Relative standard deviations of 50 Hz power loss $P$ and apparent power $S$ distributions around their reference values, obtained by comparing the measurements of INRIM, PTB, and NPL. The results obtained by an exercise on 15 different grain-oriented steel sheets performed in the year 2000 [12] are compared with the present measurements.
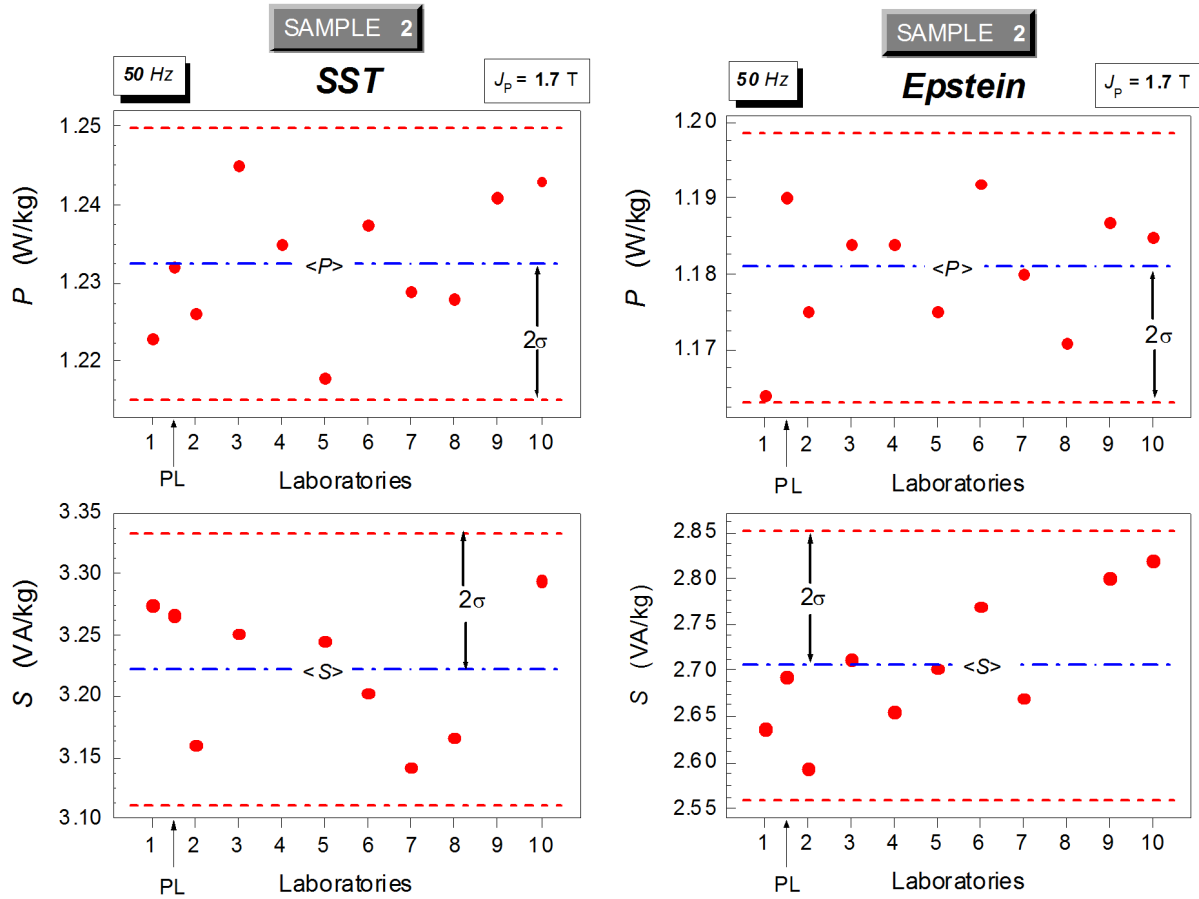
Fig. 1 – An example of scattering of the laboratories best estimates around the reference value (unweighted average, dash-dotted line). The reported values of power loss $P$ and apparent power $S$ refer to the SST and Epstein measurements in the CGO sample #2 at $J_p = 1.7$ T and $f = 50$ Hz. A few outcomes of $S$ do not appear here, because they fall outside the $\pm 2\sigma$ band around the reference value. They are discarded as outliers. The labelling of the laboratories does not correspond to the order of appearance in Table 1 (PL is the pilot laboratory).
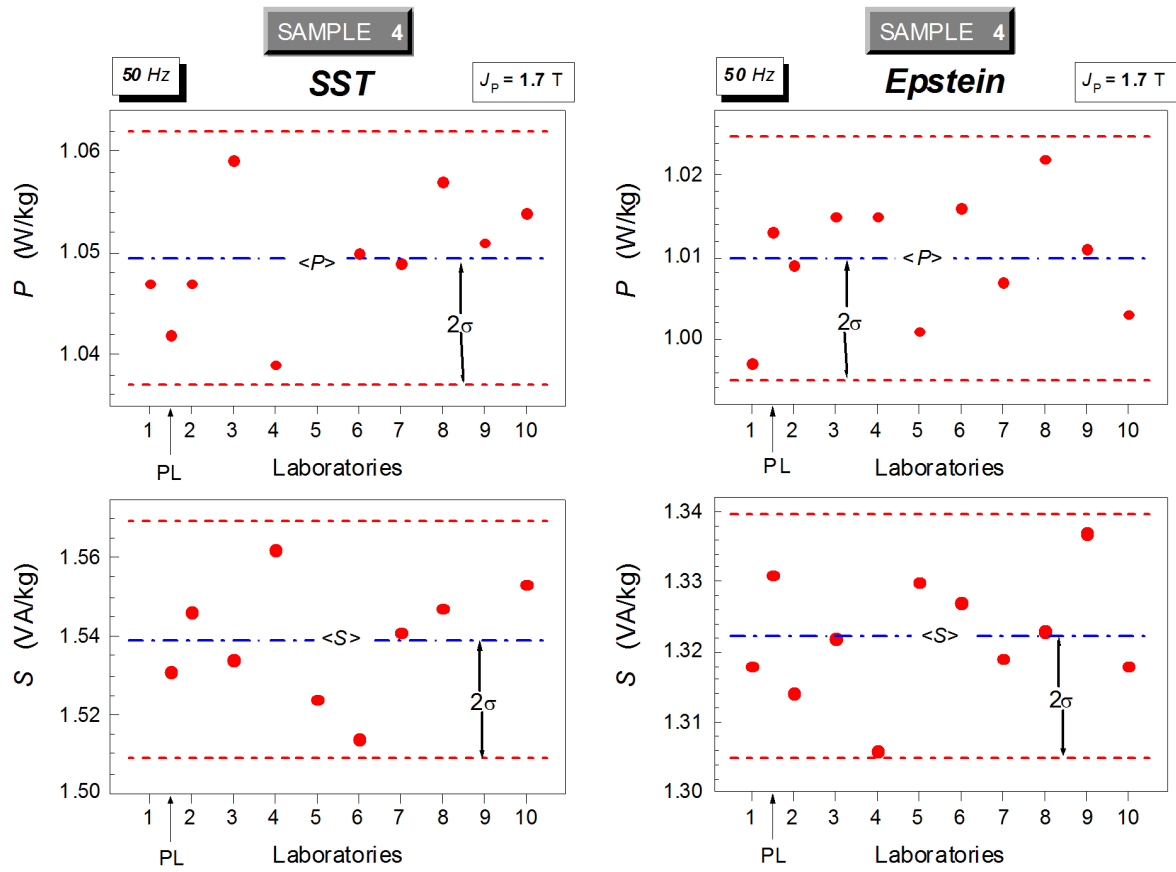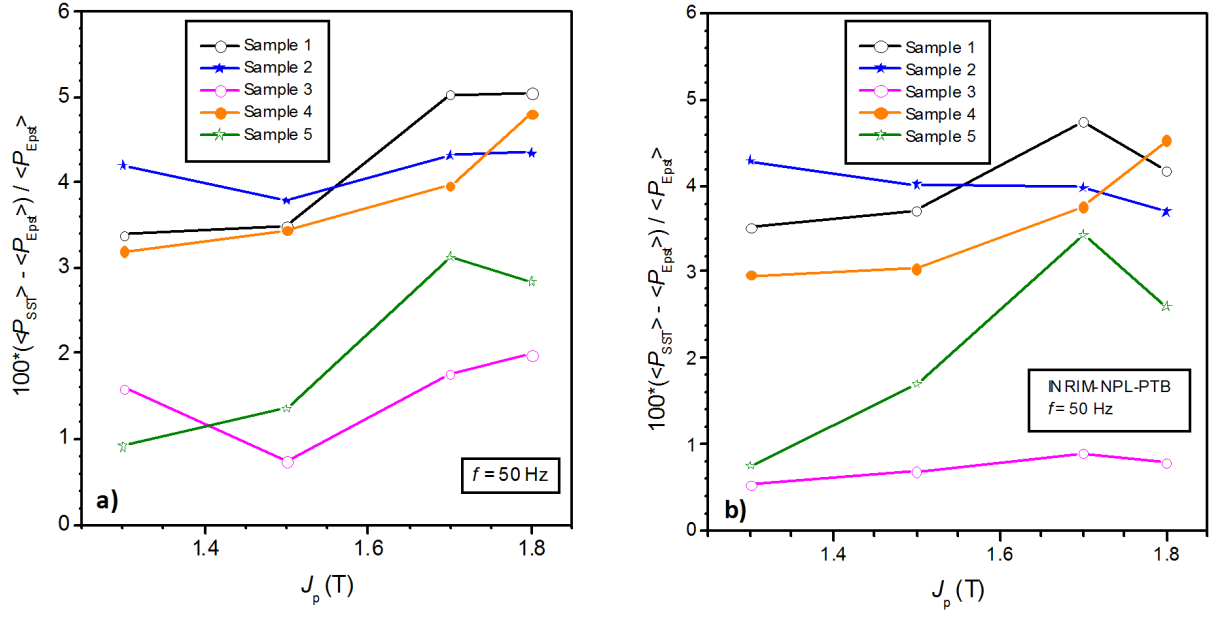
Fig. 2 – As in Fig. 1 for the HGO sample #4.

Fig. 3 – Samples #1 to #5. Ratio of SST to Epstein power loss reference values $\delta_{SE}(J_p) = (<P_{SST}> - <P_{Epst}>) / <P_{Epst}>$ at 50 Hz versus peak polarization.  a) All labs; b) the European metrological labs.

Fig. 4 – Overall dispersion of the laboratories best estimates of power loss $P_i$ and apparent power $S_i$ at 50 Hz around their reference values. The histograms show the distribution of the differences $\delta(P_i) = (P_i - <P>) / <P>$ (a) and $\delta(S_i) = (S_i - <S>) / <S>$ (b).

Fig. 5 – As in Fig. 4, with the analysis restricted to the best estimates by the European metrological labs.

Fig. 6 – Dispersion of the laboratories best estimates of SST and Epstein power losses $P_i$ at 50 Hz. The frequency $N(\delta)$ of the relative differences $\delta(P_i)$ is shown for the four investigated $J_p$ levels. The response of the HGO samples (#3, #4, #5) is separately put in evidence.

Fig. 7 – Relative standard deviations $\sigma(P)$ and $\sigma(S)$ of the distribution of the laboratories best estimates around the reference values versus peak polarization at different magnetizing frequencies.

Fig. 8 – Lab-to-lab fluctuation of the peak field value $H_p$ at $J_p = 1.3$ T (a) and  $J_p = 1.8$ T (b) for the SST and  Epstein measurements at 50 Hz.

Fig. 1 – An example of scattering of the laboratories best estimates around the reference value (unweighted average, dash-dotted line). The reported values of power loss $P$ and apparent power $S$ refer to the SST and Epstein measurements in the CGO sample #2 at $J_\text{p}$ = 1.7 T and $f$ = 50 Hz. A few $S$ outcomes do not appear here, because they fall outside the $\pm 2\sigma$ band around the reference value. They are discarded as outliers. The labelling of the laboratories does not correspond to the order of appearance in Table 1 (PL is the pilot laboratory).

Fig. 2 – As in Fig. 1 for the HGO sample #4.

Fig. 3 – Samples #1 to #5. Ratio of SST to Epstein power loss reference values $\delta_{SE}(J_p) = (<P_{SST}> - <P_{Epst}>) / <P_{Epst}>$ at 50 Hz versus peak polarization.  a) All labs; b) the European metrological labs.
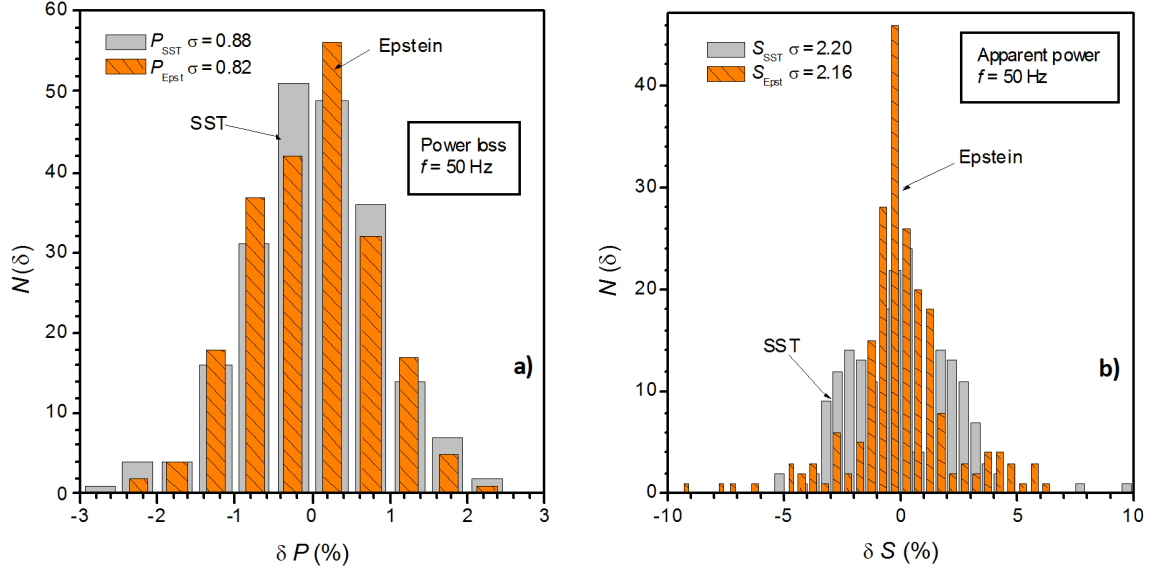
Fig. 4 – Overall dispersion of the laboratories best estimates of power loss $P_i$ and apparent power $S_i$ at 50 Hz around their reference values. The histograms show the distribution of the differences $\delta(P_i) = (P_i - <P>) / <P>$ (a) and $\delta(S_i) = (S_i - <S>) / <S>$ (b).

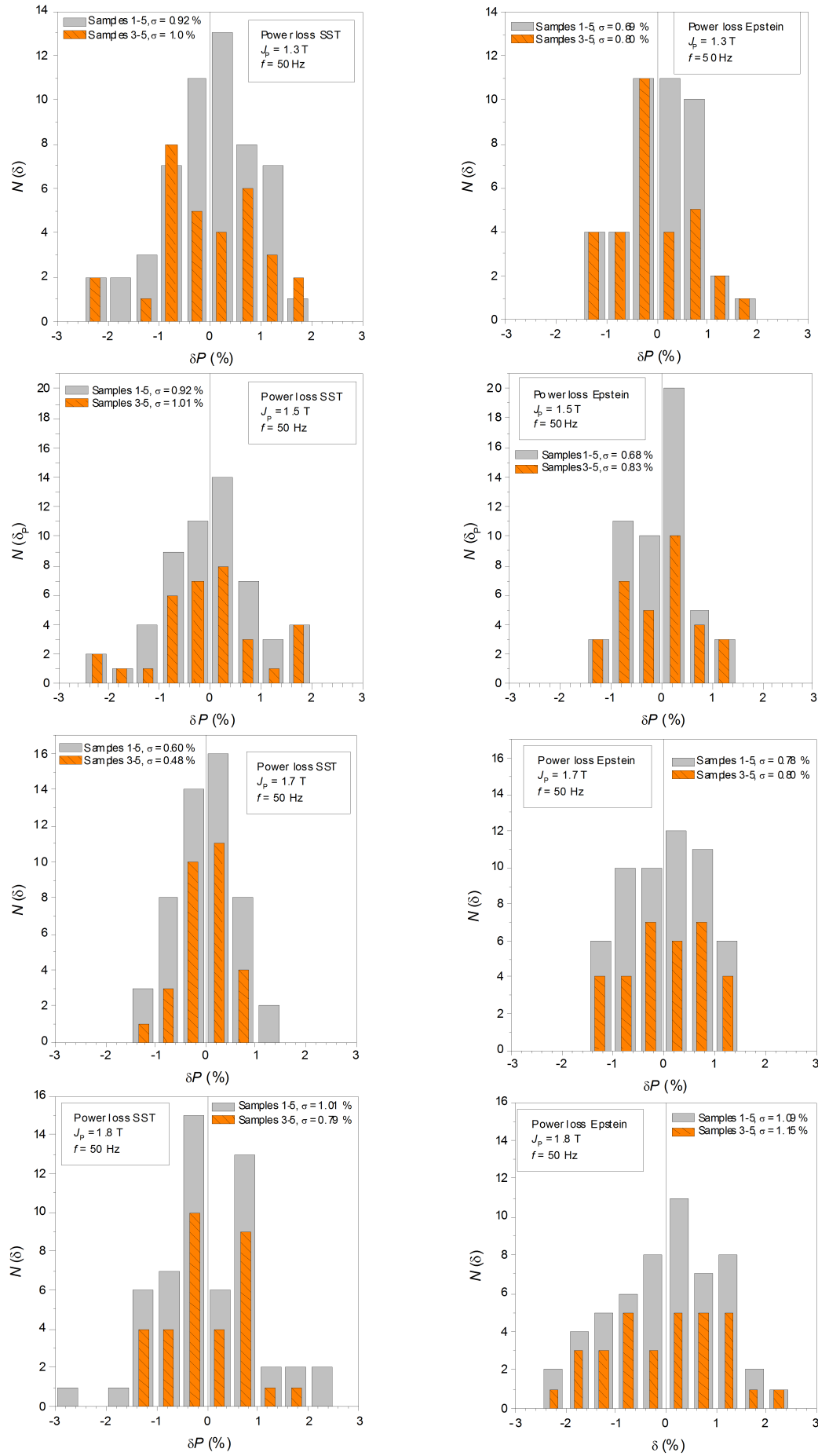Fig. 5 – As in Fig. 4, with the analysis restricted to the best estimates by the European metrological labs.

Fig. 6 – Dispersion of the laboratories best estimates of SST and Epstein power losses $P_i$ at 50 Hz. The frequency $N(\delta)$ of the relative differences $\delta(P_i)$ is shown for the four investigated $J_p$ levels. The response of the HGO samples (#3, #4, #5) is separately put in evidence.
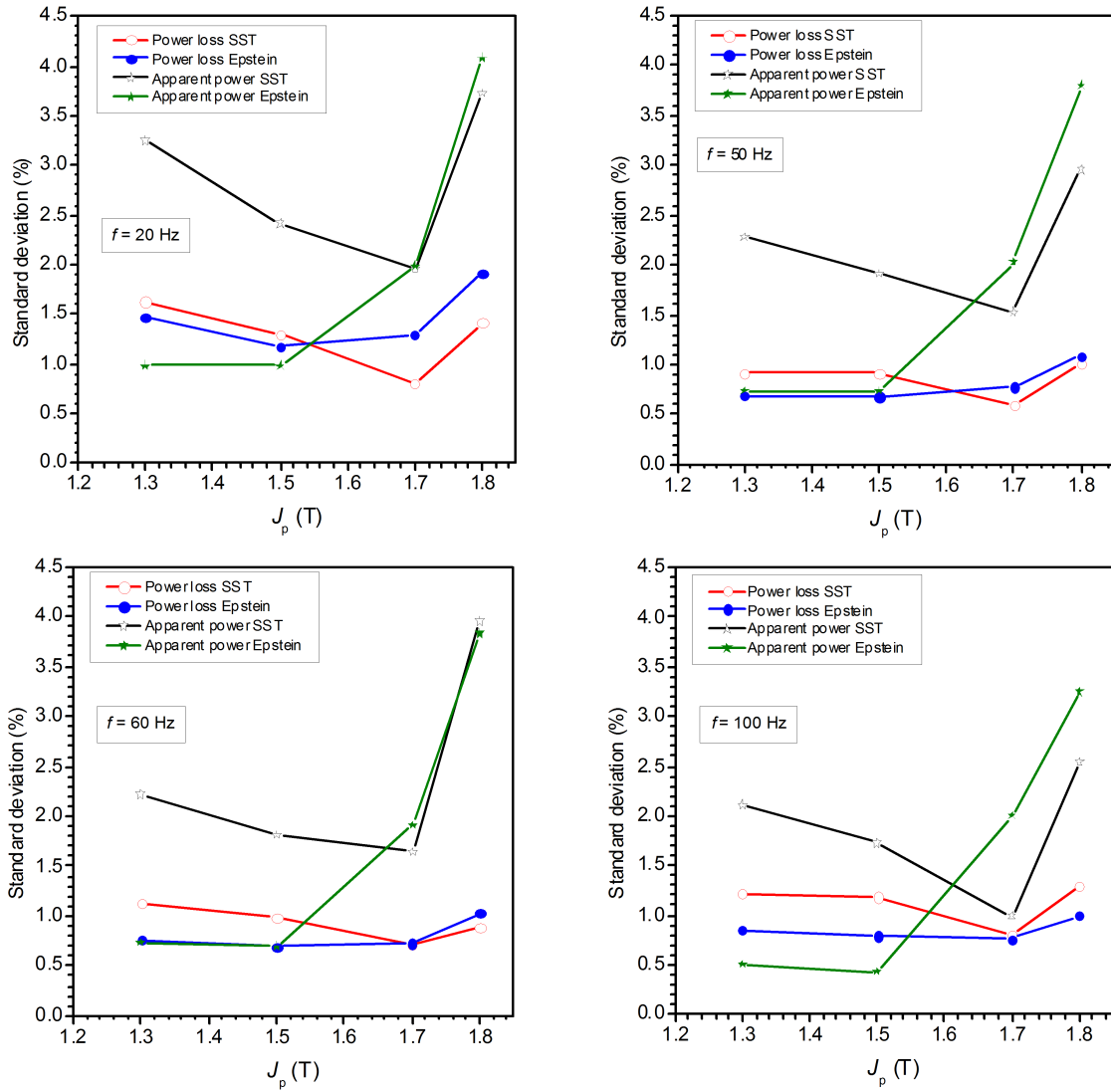
Fig. 7 – Relative standard deviations σ(*P*) and σ(*S*) of the distribution of the laboratories best estimates around the reference values versus peak polarization at different magnetizing frequencies.
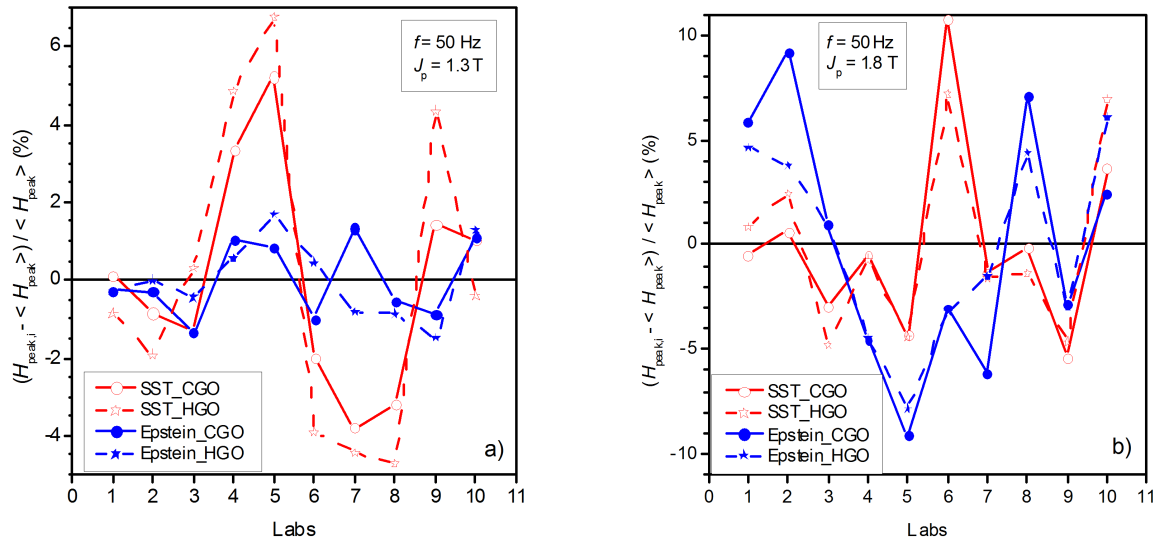
Fig. 8 – Lab-to-lab fluctuation of the peak field value $H_\mathrm{p}$ at $J_\mathrm{p}$ = 1.3 T (a) and $J_\mathrm{p}$ = 1.8 T (b) for the SST and Epstein measurements at 50 Hz.